RSC Advances

PAPER

View Article Online
View Journal | View Issue

Cite this: *RSC Adv.*, 2025, **15**, 36625

Waste robusta coffee husk pectin: ultrasound-assisted extraction and applications in roselle flower marmalade and fruit coating

Thi-Ngoc-Mai Tran,[a] Nguyen-Trung-Tien Dieu,[bc] Thi-Hong-No Nguyen,[bc] Van-Dung Le,[bc] Dinh-Tri Mai,*[bc] Chi-Hien Dang,[bc] Cao-Hien Nguyen,[d] Huynh Trong Phat[e] and Thanh-Danh Nguyen*[bc]

Received 16th July 2025
Accepted 26th September 2025

DOI: 10.1039/d5ra05086c

rsc.li/rsc-advances

This study demonstrates the valorization of robusta coffee husk as a sustainable source of pectin *via* ultrasound-assisted extraction (UAE). The optimized process yielded 16.4% pectin with favorable gelling and physicochemical properties, comparable to commercial citrus pectin. In food application, incorporation of 0.5% coffee husk pectin into roselle marmalade, together with 1.0% citric acid and 50% sucrose, produced a desirable texture and sensory quality. In packaging application, the extracted pectin was blended with chitosan to form biofilms enriched with curcumin (CPC) or pomegranate peel extract (CPP). These composite films exhibited enhanced stability and antioxidant activity, with CPP showing the strongest effect. Postharvest trials confirmed that CPP coatings extended the storage of lychee and Japanese plum by reducing weight loss and preserving texture compared to CPC and uncoated controls. This work highlights the multifunctional potential of coffee husk-derived pectin as a food ingredient and active packaging material, contributing to waste upcycling and circular bioeconomy strategies.

1 Introduction

Robusta coffee (*Coffea canephora*), one of the most widely cultivated coffee species globally, generates significant quantities of agricultural waste during post-harvest processing.[1] Coffee husks (including pulp and peel), constituting approximately 45–50% of the coffee cherry by weight, are a major byproduct and represent a growing environmental concern due to their high organic load and limited utilization pathways.[2,3] Approximately 10 million tons of coffee husk waste is discarded into the environment annually as a byproduct of the coffee industry worldwide.[4,5] Moreover, the sustainable conversion of coffee husk into value-added by-products has gained increasing attention within the circular economy framework.[6] In countries with large-scale robusta production, such as Vietnam, improper disposal of coffee husks contributes to soil acidification, water eutrophication, and greenhouse gas emissions.[7] However, these residues contain valuable bioactive compounds, notably pectin and polyphenols, which have promising applications in food science and technology.[8,9]

Pectin, a complex polysaccharide rich in galacturonic acid residues, is widely used in the food industry as a natural gelling, stabilizing, and thickening agent.[10] While conventional sources of commercial pectin include citrus peels and apple pomace, coffee husks offer a sustainable, underexplored alternative. In particular, ultrasound-assisted extraction (UAE) has emerged as an efficient, green technology for improving pectin yield and functionality from plant-based biomass.[11–14]

Roselle (*Hibiscus sabdariffa*) is a widely consumed functional plant known for its vivid red calyces, which are rich in organic acids, anthocyanins, and other phenolic compounds.[15] These bioactive constituents contribute not only to its characteristic color and tart flavor but also to its antioxidant, antihypertensive, and lipid-lowering properties.[16–18] Due to its high acid content and favorable phytochemical profile, roselle flowers are well-suited for the preparation of jams and marmalades, especially as a natural alternative to synthetic colorants and preservatives in food formulations.[19,20] The formulation of marmalade products, however, requires a suitable gelling agent to achieve the desired texture, stability, and spreadability. Pectin plays a critical role in this process, typically interacting with sugar and acid to form a stable gel network.[21] In this context, the use of pectin extracted from waste robusta coffee husks offers a novel and sustainable gelling solution. The galacturonic acid content and degree of esterification (DE) of this pectin can be tailored through extraction parameters,

[a]*Institute of Applied Sciences, HUTECH University, 475A Dien Bien Phu Street, Thanh My Tay Ward, Ho Chi Minh City, Vietnam*
[b]*Institute of Advanced Technology, Vietnam Academy of Science and Technology, Ho Chi Minh, Vietnam. E-mail: maidinhtri@gmail.com; danh5463bd@yahoo.com*
[c]*Graduate University of Science and Technology, Vietnam Academy of Science and Technology, 18 Hoang Quoc Viet, Cau Giay District, Hanoi, Vietnam*
[d]*Department of Chemical Technology, Ho Chi Minh City University of Industry and Trade, Ho Chi Minh City 700000, Vietnam*
[e]*Research Laboratories of Saigon Hi-tech Park, Lot I3, N2 Street, Saigon Hi-tech Park, Ho Chi Minh City, Vietnam*

particularly with the use of ultrasound-assisted techniques, to match the gelation requirements of high-acid fruit products, likely roselle.

Chitosan (CS), a deacetylated derivative of chitin, is widely applied in food packaging, biomedical, and agricultural fields owing to its biocompatibility, biodegradability, non-toxicity, and antimicrobial activity.[22] Its primary amino groups enable electrostatic and hydrogen-bond interactions with anionic polysaccharides such as pectin, leading to the formation of polyelectrolyte complexes.[22,23] These interactions yield composite films with enhanced film-forming ability, barrier properties, and mechanical strength. In particular, chitosan/pectin (CP) films exhibit improved integrity, flexibility, and biodegradability, making them suitable for sustainable food packaging.[23,24] Moreover, their semi-permeable structure retains moisture while permitting gas exchange, a key requirement for fresh produce coatings.[25]

Despite these advantages, CP films may still face limitations such as low bioactive activity.[26,27] To further enhance the bioactivity and functionality of CP films, recent studies have incorporated natural antioxidants and antimicrobial agents into the biopolymer matrix. Among these, curcumin, a polyphenolic compound, and pomegranate (*Punica granatum*) extract, rich in ellagitannins and anthocyanins, have attracted significant attention due to their potent antioxidant, anti-inflammatory, and antimicrobial properties.[28–30]

Curcumin, despite its health-promoting potential, suffers from low water solubility and stability under ambient conditions. However, its encapsulation or dispersion within a biopolymer film matrix can enhance its stability and facilitate its controlled release.[31,32] Chitosan, in particular, offers a favorable environment for curcumin binding through hydrogen bonding and hydrophobic interactions, while pectin contributes to matrix cohesion and film flexibility. Similarly, pomegranate extract, composed of a complex mixture of polyphenols and flavonoids, can be uniformly distributed in the CP network, providing additional antimicrobial functionality and free radical scavenging capacity.[33] The resulting bioactive CP films loaded with curcumin and pomegranate extract present a multifunctional platform for active food coatings, capable of extending shelf life and maintaining product quality. Additionally, the natural origin and safety profile of both additives support their use in edible coatings or compostable packaging.[34]

Although coffee husk represents an abundant agro-waste riching in pectic substances, previous studies on its utilization have reported low extraction yields, insufficient structural characterization, and limited demonstration of practical applications beyond basic compositional analysis.[35,36] In this study, pectin was extracted from waste robusta coffee husk *via* UAE method, with conditions optimized to enhance yield and functionality. The pectin was characterized and applied as a gelling agent in roselle (*Hibiscus sabdariffa*) marmalade, and as a film-forming biopolymer in edible coatings enriched with curcumin and pomegranate extract, targeting lychee (*Litchi chinensis*) and Japanese plum (*Prunus salicina*). These bioactive films were evaluated for structural and functional properties to support fruit preservation. The study offers a sustainable strategy for agro-waste valorization and bio-based material development within a circular economy context.

2 Materials and methods

2.1 Materials

The robusta coffee (*Coffea canephora*) husk was collected from Dak Lak province, Vietnam. The scientific name of the plant was authenticated by the botanist Dang Van Son, Institute of Tropical Biology, Vietnam Academy of Science and Technology. The husk samples were washed with cold tap water, followed by with distilled water. Then the husks were dried to remove any moisture. The dried husks were milled and the resulting powder was stored in low-density polyethylene bags at room temperature for further uses. Moisture content of dried husks was determined to be 13.57 ± 0.18%.

Chemicals including NaOH, phenolphthalein, starch, HCl, citric acid, sodium acetate, acetic acid, $CaCl_2$, NaCl purchased from Xilong, China. Ethanol (96%) obtained from Vietchem Co., Vietnam were used as chemical reagents. Chitosan with molecular weight of 100 000–300 000 was purchased from Thermo Scientific (USA). Curcumin (95%) was purchased from Oxford Lab Fine Chem (India). Distilled water was used thoroughly. Commercial lemon and orange peel high methoxyl pectin with DE > 50% (Cargill, Incorporated, USA) required a high soluble solids content (above 60%) and a low pH (2.8–3.5) to form a gel, was used in the production of gummy candies and firm jams.

Raw material processing method: roselle (*Hibiscus sabdariffa*) calyces were washed, then ground with water at a 1 : 1 ratio to form a paste. The resulting mixture was filtered to remove solid residues, and the clear filtrate was collected for further use. Hardness measurements were performed using a texture analyzer (ZwickRoell, Germany). Sensory evaluation by quality scoring analysis method (TCVN 3215:1979). The color of food samples was determined using a colorimeter (Chroma Meter CR-400, Minolta, Japan). Determination of acidity by acid–base titration method (TCVN 5483-2007).

Pomegranate peel extract was prepared following the previous method[37] with slight modifications. Briefly, dried pomegranate peel was combined with distilled water at a solid-to-liquid ratio of 1 : 10 (w/v) and extracted using microwave-assisted treatment at 800 W for 15 minutes. The resulting mixture was centrifuged, and the supernatant was concentrated under reduced pressure using vacuum evaporation. The concentrated extract was stored in amber bottles at room temperature (25 ± 2 °C) until further use. The extraction yield was 24.8% (w/w), and the total polyphenol content was determined to be 450.3 ± 13.5 mg gallic acid equivalents (GAE) per gram of extract.

2.2 Ultrasound-assisted extraction of pectin from coffee husk

2.2.1 Heating extraction. 5 g of coffee husk powder were placed into an Erlenmeyer flask (250 mL) containing citric acid

extraction solution (100 mL) with the pH adjusted to 2.0. The mixture was heated at 85 °C for 120 minutes and ethanol was added to the extract. The precipitate was filtered and washed several times with ethanol (96%). The collected precipitate was dried at 60 °C for 20 hours.

2.2.2 Ultrasound-assisted extraction using ultrasonic cleaning bath. 5 g of coffee husk powder were placed into an Erlenmeyer flask (250 mL) containing citric acid extraction solution (100 mL) with the pH adjusted to 2.0. The flask was placed in an ultrasonic cleaning bath, with the temperature set at 50 °C for 30 minutes. Ethanol was added to the citric acid extract. The precipitate was filtered and washed several times with ethanol (96%). The collected precipitate was dried at 60 °C for 20 hours.

2.2.3 Ultrasound-assisted extraction of coffee husk pectin using ultrasonic homogenizer. 5 g of coffee husk powder were placed into a cylindrical glass tube (250 mL) containing citric acid extraction solution (100 mL) with the pH adjusted to 2.0. An ultrasonic homogenizer probe at ultrasonic frequency of 20 kHz was immersed 2 cm into the solution in the glass tube. UAE was conducted using the optimized amplitude (20–35%), temperature (40–70 °C), and time (5–20 min) conditions. Ethanol was added to the extract. The precipitate was filtered and washed several times with ethanol (96%). The collected precipitate was dried at 60 °C for 20 hours. All experimental procedures were conducted in triplicate.

2.2.4 Degree of esterification (DE). Degree of esterification (DE) was determined *via* a previous method.[38] Briefly, pectin sample (0.5 g) was dispersed in a 250 mL beaker with 5 mL ethanol, 1 g NaCl, and 1–2 drops of phenolphthalein. After adding 100 mL of warm water and mixing thoroughly, the solution was titrated with NaOH solution (0.1 N) to the first persistent pink endpoint (V_1). Next, 25 mL of NaOH solution (0.25 N) was added, and the mixture was left at room temperature for 30 min for saponification. The excess alkali was neutralized with 25 mL of HCl solution (0.25 N), and the solution was titrated again with NaOH solution (0.1 N) to the second pink endpoint (V_2). The degree of esterification (DE) is calculated using eqn (1).

$$\mathrm{DE}\ (\%) = \frac{V_2}{V_1 + V_2} \times 100\% \quad (1)$$

where V_1 is the volume of NaOH (0.1 N, mL) consumed to neutralize free carboxyl groups, and V_2 is the volume of NaOH (0.1 N, mL) consumed to neutralize the carboxyl groups released after saponification of esterified groups.

2.3 Preparation of roselle marmalade using coffee husk pectin

Roselle calyces (100 g) were deseeded, washed, and cut into 1 cm pieces. The prepared samples were heated with 200 mL of water at varying temperatures (80–90 °C) for different times (2–4 minutes). The heated mixture was subsequently blended and passed through a 0.5 mm mesh sieve to obtain a smooth puree. The puree was then formulated with different concentrations of citric acid, sugar, and pectin. The pectin concentrations investigated were 0.5%, 1.0%, 1.5%, and 2.0%, while sugar levels were adjusted to 40%, 45%, 50%, and 55%. Citric acid was incorporated at concentrations of 0.5%, 1.0%, 1.5%, and 2.0%. To evaluate the effectiveness of coffee husk pectin, commercial citrus-derived pectins, including orange and lemon peel pectin, were also used for comparison. The mixture was concentrated to achieve a total soluble solids content of 60–65° Brix, followed by hot filling. The final product was then pasteurized at 90 °C and stored in a controlled freezing chamber at 18–20 °C for 24–48 hours.

2.4 Analytical methods of roselle marmalade

2.4.1 Color analysis. The color of food samples was determined using a colorimeter (Chroma Meter CR-400, Minolta, Japan). The color attributes L^*, a^*, and b^* were recorded to evaluate the sample color. Here, L^* indicates lightness, a^* represents the transition from red to green, and b^* denotes the transition from yellow to blue. The total color difference (ΔE) was calculated by eqn (2).

$$\Delta E = \sqrt{\left(L_0^* - L^*\right)^2 + \left(a_0^* - a^*\right)^2 + \left(b_0^* - b^*\right)^2} \quad (2)$$

where, L_0^*, a_0^* and b_0^* represent the color parameters of the sample on day 0 (before storage) while L^*, a^*, and b^* are measured on the analysis day.

2.4.2 Hardness profile analysis. The hardness of jam samples was determined using a Texture Analyzer (ZwickRoell, Germany) equipped with a TA44 cylindrical probe. Samples were molded into uniform blocks (15–20 mm in height and 20–25 mm in width/diameter) and equilibrated at room temperature prior to testing. The instrument was calibrated by zeroing the load (0 N) and probe position (zero distance), followed by verification of load cell sensitivity. Test parameters were set in the TestXpert software as follows: pre-test speed, 1.0 mm s^{-1}; trigger force, 0.05 N; test speed, 1.0–2.0 mm s^{-1}; deformation distance, 30–50% of sample height; and post-test speed, 1.0 mm s^{-1}. During measurement, the probe descended until the trigger force was detected, compressed the sample to the defined deformation, and subsequently withdrew. For Texture Profile Analysis (TPA), a two-cycle compression was applied with a short interval between cycles. Force–distance curves were recorded, and hardness was expressed as the maximum force (N) during the first compression cycle. Each measurement was performed in triplicate, and mean values were reported.

2.4.3 Sensory evaluation. The sensory properties of the marmalade samples were evaluated by 20 panelists. Each sample (20 g) was served on a paper plate. Panelists were instructed to refrain from consuming any food for at least 30 minutes prior to the evaluation. They were asked to assess the color, aroma, flavor, and texture (including toughness and breaking strength), as well as the overall acceptability of the samples. A 5-point hedonic scale was used to rate their preference, where 1 = strongly dislike, 2 = dislike, 3 = neither like nor dislike, 4 = like, and 5 = strongly like.[39]

2.5 Preparation of biofilm

Biofilms comprising coffee husk pectin and chitosan were prepared following a previous methodology,[27] with minor

modifications. Briefly, pectin powder (2 g) were dissolved in 50 mL of distilled water, while chitosan (1 g) was dissolved in 50 mL of acetic acid solution (1%). The two solutions were then combined at a 1 : 1 volume ratio (v/v). The mixture was typically maintained at a pH range of 3.5–4.5. Glycerol was incorporated at 40% (w/w) as a plasticizer, and the resulting mixture was continuously heated at 70 °C for 120 minutes to achieve homogeneity. The homogeneous chitosan/pectin (CP) solution was cast into the mold and dried at 60 °C for 24 hours.

For functionalized films, curcumin (0.1%, w/w) or pomegranate peel extract (1%, w/w) was added to CP solution prior to casting, yielding chitosan/pectin/curcumin (CPC) and chitosan/pectin/pomegranate peel extract (CPP) films, respectively. Upon completion of the drying process, the biofilms were carefully peeled from the Petri dishes and stored in a desiccator until further analysis and application.

2.6 Physicochemical characterizations

2.6.1 Measurement. Surface measurements were conducted using an optical microscope with iphone 10 (Carson Micro-Mini 20× Pocket Microscope) at a magnification of 10×.

The morphological characteristics were examined using a scanning electron microscope (SEM) (Hitachi Fe-SEM S4800, Tokyo, Japan). Images were captured at an accelerating voltage of 10.0 kV with magnifications of 40× and 5000×.

Fourier-transform infrared spectroscopy (FTIR) (Bruker Tensor 27, Germany) was used to analyze functional groups over a wavelength range of 450–4000 cm^{-1}.

^1H NMR (Brucker Advance NEO_600 MHz, D_2O) were measured to identify the pectin structure.

Molecular weight (MW) distribution of coffee husk pectin was determined by GPC using a Hewlett–Packard 1050 HPLC system (Agilent Technologies, USA) equipped with an ELSD detector. Separation was performed on a Shodex KB-804 column with deionized water as the mobile phase at a flow rate of 1.0 mL min^{-1} and an injection volume of 20 μL. ELSD parameters were set at 35 °C (nebulizer), 70 °C (evaporator), and N_2 flow at 1.8 mL min^{-1}. Samples were dissolved in water (1 mg mL^{-1}), filtered through 0.22 μm membranes, and injected in duplicate. Calibration was achieved with a series of pullulan standards (MW 5–800 kDa) and glucose. M_n, M_w, and polydispersity index (PDI) were calculated from the calibration curve.

2.6.2 Swelling ratio and water solubility of biofilms. The swelling ratio was determined following the method outlined by Jiatong Yan *et al.*,[40] with minor modifications. Biofilms were cut into squares measuring 20 mm × 20 mm to record their initial mass. The samples were then exposed to the environment to allow natural swelling. After swelling, the biofilms were weighed and the swelling ratio was calculated by eqn (3).

$$\text{Swelling ratio } (\%) = \frac{m_1 - m_0}{m_0} \times 100\% \quad (3)$$

where, m_0 and m_1 is the mass of biofilm before and after swollen films, respectively.

To study water solubility, the water solubility of the biofilm was assessed based on a previous method,[41] with slight modifications. The biofilms dried in an oven at 105 °C for 8 hours were cut into 3–5 cm pieces and weighed to determine their initial dry mass. Each sample was immersed in a beaker containing 30 mL of distilled water and incubated at room temperature for 24 hours. After incubation, the biofilm was removed and dried again at 105 °C for 8 hours. Water solubility was calculated using eqn (4).

$$\text{Water solubility } (\%) = \frac{m_0 - m_1}{m_0} \times 100\% \quad (4)$$

where m_0 and m_1 are weight of the initial biofilm and final weight after the drying process.

2.6.3 Water vapor permeability. Water vapor permeability (WVP) was carried out by a previous method,[42] with slight modifications. This method was designed to assess the capability of the pectin-chitosan biofilms to inhibit water vapor transmission. To conduct the experiment, a test tube containing dry silica gel (10 g) was sealed with the biofilm and placed in a desiccator filled with distilled water. The setup was maintained at a constant temperature of 32 °C. The increase in the tube's weight was recorded every 24 hours. The WVP value of each biofilm was calculated using the following eqn (5).

$$\text{WVP } \left(\text{g mm}^{-1}\ \text{s}^{-1}\ \text{Pa}^{-1}\right) = \frac{w \times x}{A \times t \times (P_2 - P_1)} \quad (5)$$

where w is the weight loss of the test tube (g) over the duration of the time t (s); x is the tested biofilm's thickness (m); A is the testing biofilm's exposed area (m^2); (P_2–P_1) is the water vapor pressure differential over the biofilm under test (Pa). For the blank, a tube containing 10 g of silica was used without sealing it with the biofilm.

2.7 Antioxidant activity of biofilms

2.7.1 DPPH method. The antioxidant activity of the biofilms was determined using the 2,2-diphenyl-1-picrylhydrazyl (DPPH) assay, based on the reduction of the stable DPPH free radical exhibiting an absorption maximum at 517 nm.[43] Briefly, a biofilm sample with an area of 1.0 cm^2 was immersed in 5.0 mL of an ethanolic DPPH solution (0.05 mM). The mixture was gently agitated at room temperature for 30 minutes in the dark to prevent photo-induced degradation. After incubation, the absorbance was recorded at 517 nm using a spectrophotometer. A control used ethanol under the same conditions. The radical scavenging activity (RSA) was calculated according to the following eqn (6).

$$\text{RSA } (\%) = \frac{A_0 - A_1}{A_0} \times 100 \quad (6)$$

where A_0 and A_1 is the absorbance of the control and sample, respectively.

2.7.2 Hydrogen peroxide scavenging assay. The hydrogen peroxide scavenging assay was performed as described by a previous method with minor modifications.[44] Briefly, 0.25 mL of ferrous ammonium sulfate (1 mM) was mixed with 1.5 mL of the sample. Next, 62.5 μL of hydrogen peroxide (5 mM) was added, and the mixture was incubated at room temperature in the dark for 5 minutes to prevent hydrogen peroxide photobleaching. After incubation, 1.5 mL of 1,10-phenanthroline (1

mM) was added to the mixture, which was thoroughly mixed and left to stand at room temperature for 10 minutes. The absorbance was measured at 510 nm using a spectrophotometer. A blank solution, comprising 1.5 mL of 1,10-phenanthroline (1 mM), 1.562 mL of water, and 0.25 mL of ferrous ammonium sulfate (1 mM), was prepared, and its highest absorbance value was used as a reference. The hydrogen peroxide scavenging capacity of the biofilms was calculated using eqn (7).

$$\%\ H_2O_2\ \text{scavenging activity} = \frac{A_{\text{Sample}}}{A_{\text{Blank}}} \times 100 \quad (7)$$

2.8 Fruit coating

The preservation ability of biofilms was carried for life of lychee (*Litchi chinensis*) and Japanese plum (*Prunus salicina*). Solutions of CP, CPC, and CPP were prepared for the experiment, utilizing pesticide-free, thoroughly washed, and clearly labeled *Litchi chinensis* and *Prunus salicina*. Each sample was immersed in the prepared solutions and air-dried on a rack at room temperature to ensure no risk of biofilm contamination. After drying for 24 hours, the samples were gently wrapped in biofilm to simulate the "shipping environment" typically encountered during export, following the previous method.[45] The change in sample mass after 24 hours was calculated using eqn (8).

$$\text{Mass reduction}\ (\%) = \frac{m_0 - m_t}{m_0} \times 100\% \quad (8)$$

where m_0 (g) is the initial mass of the fresh fruit at day 0, and m_t (g) is the mass of the same fruit at each time interval.

2.9 Statistical methods

All experimental procedures were conducted in triplicate, and the mean values were used for reporting and analysis. Statistical differences among the results were evaluated using analysis of variance (ANOVA) at a 95% confidence level ($p \leq 0.05$). Data analysis was performed using Statgraphics software.

3 Results and discussion

3.1 Optimizing ultrasound extraction

Fig. S1 illustrates that ultrasound-assisted extraction (UAE) significantly enhances pectin yield compared to conventional thermal methods. Specifically, thermal extraction at 85 °C for 2 hours yielded 7.8 ± 2.6%, whereas the UAE method using an ultrasonic bath at 50 °C for only 30 minutes produced a higher yield of 10.2 ± 2.5%. Remarkably, the use of an ultrasonic probe within 10 min further increased the yield to 16.4 ± 2.4%. These findings underscore the efficiency of ultrasound technology in maximizing pectin recovery while markedly shortening extraction time from coffee husk residues. The lower yield observed with the ultrasonic bath is likely due to the indirect application of ultrasonic energy, where sound waves are partially attenuated by the liquid medium. In contrast, the ultrasonic probe delivers direct and intense mechanical energy, effectively disrupting the plant cell wall and membrane structures. This mechanical disruption enhances solvent penetration and facilitates the release of intracellular pectin, demonstrating the advantage of ultrasonic homogenization in extraction processes. The yield obtained from robusta coffee husk pectin is lower than that of citrus pectin (12.93–29.05%)[46] but remains valuable due to the rapid and environmentally friendly extraction achieved through ultrasound technology.

FTIR spectra recorded in the infrared region (450–4000 cm^{-1}) were utilized to identify the functional groups present in the extracted pectin samples (Fig. S1B). Despite differences in extraction methods, all spectra displayed similar characteristic bands, indicating a consistent chemical structure among the samples. A broad absorption band at 3434 cm^{-1} corresponds to O–H stretching vibrations, while peaks at approximately 2950 and 2750 cm^{-1} are associated with the C–H stretching of methyl ester groups (O–CH_3) within esterified galacturonic acid units. Carboxylate groups were evident through an asymmetric stretching band around 1627 cm^{-1} and a weaker symmetric band near 1410 cm^{-1}. Additionally, strong absorptions in the 1740 and 1627 cm^{-1} region were attributed to the stretching vibrations of carbonyl (C═O) and carboxylate (COO^-) groups.

Notably, the intensity and area of the ester carbonyl absorption bands increased with rising degree of esterification (DE), while the corresponding carboxylate peaks showed a marked decline. Pectin extracted by conventional reflux displayed a significantly lower DE compared to UAE, likely due to prolonged acid exposure during thermal processing, which promotes ester bond hydrolysis. This lower DE may enhance pectin solubility in aqueous media, leading to reduction of extraction efficiency. In contrast, pectin obtained *via* ultrasound homogenization exhibited higher DE values, suggesting better suitability for gelation in roselle flower marmalade and improved integration into CP biofilms. Despite differences in extraction conditions, all samples presented comparable FTIR spectral features, indicating preservation of key functional groups and a consistent core chemical structure across methods.

The modeling strategies employed in pectin extraction primarily consider hydrolysis, diffusion, and degradation processes occurring within a homogeneous medium. These models may describe individual mechanisms or a combination thereof, depending on the complexity of the system. The choice and applicability of a given model are closely linked to the extraction technique used, including the type of solvent and method applied. A comprehensive understanding of these models allows for accurate prediction of extraction behavior on a phenomenological level.

To gain further insights into the extraction process, morphological analyses of raw materials, before and after treatment, are often conducted. In this study, structural changes in both the extracted pectin and the residual husk were evaluated using optical microscopy and scanning electron microscopy (SEM), as illustrated in Fig. 1. The findings revealed pronounced alterations in surface morphology following all extraction techniques. Optical microscopy indicated evident differences in color and structure compared to untreated husks.

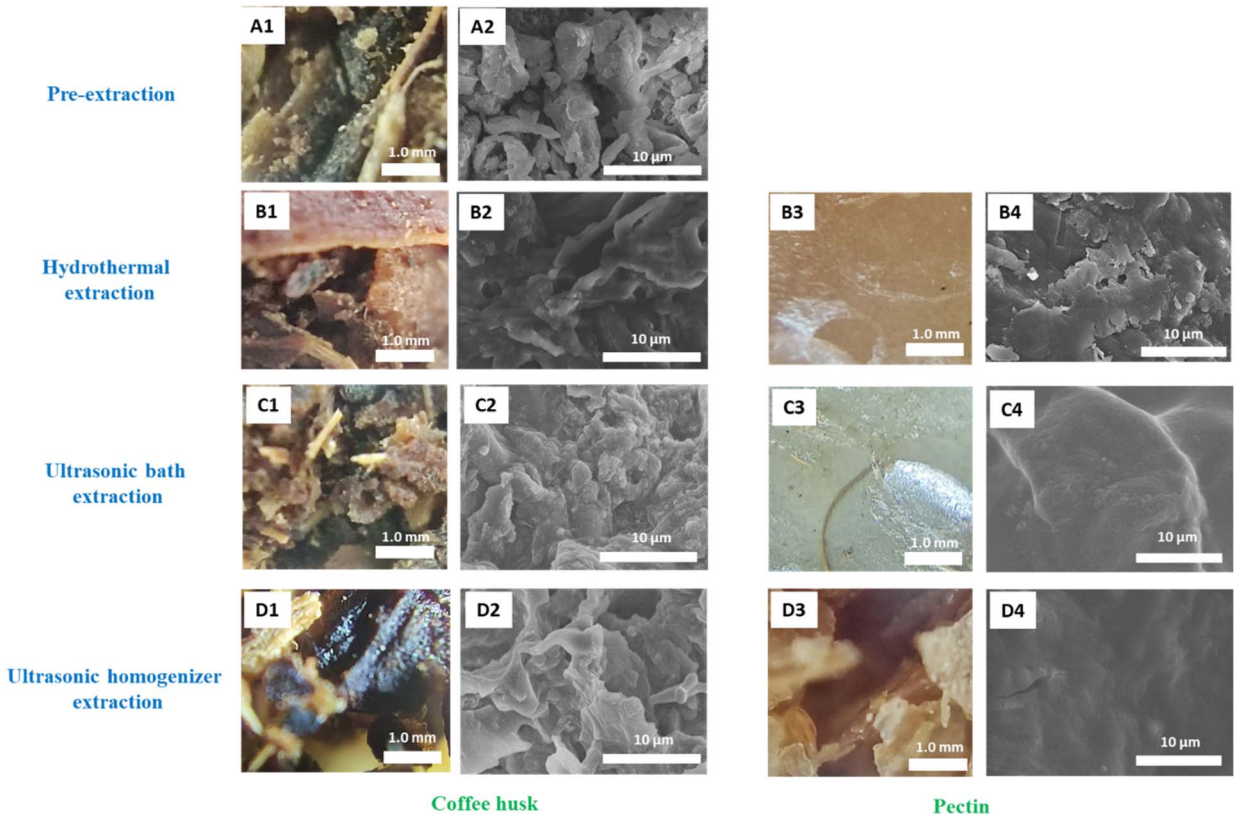

Fig. 1 Microscopy and FE-SEM images of coffee husk and pectin under different treatments. (A1 and A2) Pre-extraction coffee husk; (A3 and A4) pre-extraction pectin. (B1–B4) Hydrothermal extraction: coffee husk (B1 and B2) and pectin (B3 and B4). (C1–C4) Ultrasonic bath extraction: coffee husk (C1 and C2) and pectin (C3 and C4). (D1–D4) Ultrasonic homogenizer extraction: coffee husk (D1 and D2) and pectin (D3 and D4).

SEM analysis of the raw coffee husk displayed irregularly shaped particles, typically between 0.5 and 5.0 μm, with distinct edges and layered arrangements. Post-extraction, these particles showed considerable disintegration, reflecting significant cell wall damage.

Among the methods tested, UAE, especially with the use of an ultrasonic homogenizer, resulted in the most extensive cell disruption. While optical microscopy did not distinguish substantial differences between the ultrasonic bath and probe treatments, SEM images highlighted more severe rupture in samples treated with the ultrasonic homogenizer (Fig. 1C2 and D2). This heightened disruption likely underpins the increased pectin yield observed with this method.

The morphological characteristics of pectin obtained from coffee husk extraction provide valuable insights into the extraction process (Fig. 1). Microscopy images (Fig. 1B3, C3, and D3) indicate that both hydrothermal and ultrasound-assisted extraction methods yield pectin films with superior structural integrity compared to those produced using ultrasonic homogenization. The films extracted by hydrothermal and ultrasound bath-assisted methods exhibit more uniform surfaces with fine striations, whereas the pectin films obtained *via* ultrasonic homogenization appear disrupted. This degradation confirmed the higher DE observed in pectin extracted by ultrasonic homogenization, which could hinder film formation. However, SEM analysis reveals that the microstructure of pectin from ultrasonic extraction appears more stable than that of the hydrothermal extraction. These observations clearly demonstrate that the extraction method significantly influences the physicochemical properties of the resulting pectin. Furthermore, compared to conventional thermal extraction, ultrasound homogenization techniques offer several advantages, including higher yield, lower energy consumption and reduced solvent usage. Operating under relatively mild temperature conditions, ultrasound-assisted extraction helps preserve the native structure and functional properties of pectin, potentially enhancing the quality of the final product.

3.2 Optimization of ultrasound-homogenization extraction parameters

To optimize the UAE process, the effects of amplitude, temperature, and extraction time on pectin yield, purity, and DE value were systematically evaluated. As illustrated in Fig. 2A, both yield and purity increased as the amplitude rose from 20% to 25%. At 20% amplitude, the yield, purity, and DE were 12.1 ± 0.68%, 50.2 ± 0.61%, and 67.3 ± 0.64%, respectively. These values increased to 16.2 ± 0.18%, 51.4 ± 0.07%, and 69.8 ± 0.64% at 25% amplitude. However, further increases in amplitude led to a decline in both yield and purity. This behavior can be attributed to enhanced cavitation effects at moderate amplitudes, where the collapse of microbubbles generates high

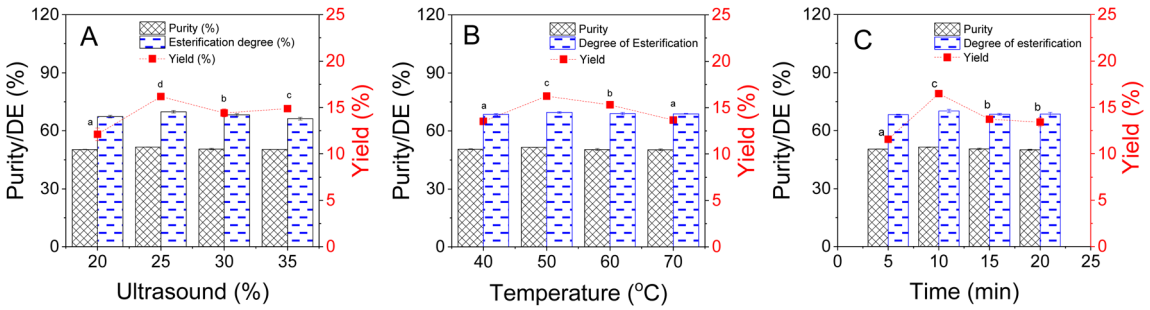

Fig. 2 Effect of ampilitude (A), temperature (B) and time (C) on purity, degree of esterification, and extraction yield using ultrasonic homogenizer. Different letters indicate statistically significant differences between samples ($P < 0.05$).

localized temperatures and pressures, facilitating cell disruption and improving the release of intracellular pectin.[47] At excessively high amplitudes, the formation of an excessive number of cavitation bubbles may hinder energy transmission due to bubble coalescence and damping effects, thereby reducing extraction efficiency.[48] Based on these findings, an amplitude of 25% was selected for subsequent experiments.

Fig. 2B demonstrates that extraction yield was significantly affected by temperature, whereas purity and DE remained relatively stable. The yield increased from 13.5% at 40 °C to 16.2% at 50 °C, followed by a significant decrease to 13.7% at 70 °C. Throughout this temperature range, purity and DE values remained approximately 50.5% and 69.5%, respectively. Higher temperatures reduce the surface tension and increase the vapor pressure inside bubbles, thereby inhibiting cavitation collapse and lowering the energy released during cavitation events. This reduces cell wall disruption and mass transfer efficiency, ultimately decreasing extraction yield.[49] Furthermore, pectin degradation may occur at elevated temperatures, leading to a reduction in pectin content. Consequently, 50 °C was chosen as the optimal extraction temperature.

The influence of extraction time on pectin yield and quality is presented in Fig. 2C. Both yield and purity increased with extraction time from 5 to 10 minutes, reaching maximum values of 16.4% and 51.3%, respectively, at 10 minutes. Further extension to 15 minutes resulted in a decrease in both parameters. Similarly, DE increased from 66% at 5 minutes to 70% at 10 minutes, remaining consistently above 50%, confirming the extracted pectin as high methoxyl pectin. Thus, optimal extraction conditions were established at 25% amplitude, 50 °C, and 10 minutes extraction time. During UAE process, the interaction between solvent and plant tissue is greatly influenced by the extraction time. Adequate sonication enhances solvent diffusion and promotes the disruption of cell membranes, facilitating the release of pectic substances.[22] However, prolonged ultrasonication may lead to degradation of pectin molecules into lower molecular weight fractions, thereby reducing both yield and purity.

Ultrasound-assisted extraction generates strong cavitation effects that can cause depolymerisation, molecular weight reduction, and demethylation in pectin, thereby altering its gelling capacity and interactions with other biopolymers.[50,51] Under the optimized conditions (25% amplitude, 50 °C, 10 min), these effects enhance mass transfer and yield while limiting excessive degradation. From an industrial perspective, UAE is attractive due to its short processing time, reduced solvent use, and mild conditions compared to conventional heating. The ability to obtain high yield and purity within a few minutes at moderate temperature underscores its energy efficiency and potential to reduce operational costs. Although scale-up requires investment in high-power ultrasonic reactors and continuous-flow systems, techno-economic studies indicate that the initial capital cost can be offset by long-term savings in energy, solvents, and processing time.[48,52] Thus, UAE represents a promising approach for sustainable, large-scale pectin production.

Fig. S2 illustrates the influence of various drying temperatures and durations on the moisture content and color attributes of coffee husk-derived pectin. The moisture content ranged from a maximum of 16.55% (50 °C for 8 h) to a minimum of 9.65% (90 °C for 20 h), indicating a clear inverse relationship between drying severity and residual moisture. Similarly, both increasing temperature and extended drying time led to a progressive decline in the L^* value, indicating darker coloration of the pectin samples. For instance, pectin dried at 50 °C for 8 h exhibited color values of $L^* = 55.59 \pm 0.57$, $a^* = 7.15 \pm 1.24$, and $b^* = 9.33 \pm 0.44$, whereas drying at 80 °C for 8 h yielded $L^* = 47.52 \pm 0.48$, $a^* = 8.42 \pm 0.97$, and $b^* = 8.10 \pm 1.09$.

The L^* parameter, representing lightness in the CIE Lab* color space, serves as a critical indicator of visual and perceived product quality. Higher L^* values correspond to lighter-colored pectin and are associated with minimal thermal degradation, thereby preserving the native molecular structure. In contrast, reduced L^* values reflect pronounced thermal degradation and potential formation of dark-colored byproducts, adversely affecting both aesthetic quality and market appeal. Correspondingly, the total color difference (ΔE) between samples was substantial – 27.74 ± 0.66 for 50 °C for 8 h and 20.58 ± 1.49 for higher temperature treatments – exceeding the perceptibility threshold ($\Delta E > 5$) and confirming visible color variation to the human eye.

Moisture content also decreased consistently with elevated drying temperature and prolonged exposure, aligning with the thermal-driven removal of bound water. Notably, all samples

achieving moisture content below 12%, including those dried at 50 °C for 20 h, 70 °C for 16–20 h, and 90 °C for 16–20 h, met the threshold required by TCVN 12100:2017 standards. Among them, the sample dried at 50 °C for 20 h exhibited the highest L^* value, indicating superior lightness and minimal discoloration. This condition was therefore identified as optimal, balancing sufficient dehydration with favorable color retention, and producing high-quality pectin with desirable visual characteristics.

The chemical structure and molecular weight (MW) distribution of the extracted coffee husk pectin were investigated using ^{1}H-NMR and GPC analysis, as illustrated in Fig. S3. The GPC chromatogram revealed a bimodal distribution, with two main peaks appearing at retention times of 5.027 and 5.574 min, corresponding to molecular weights of 1738 kDa (PDI 0.929) and 652 kDa (PDI 0.948), respectively. This suggests that the extracted pectin contained both high-molecular-weight and medium-molecular-weight fractions, which may arise from variations in chain length or partial depolymerization during extraction. The relatively low PDI values (<1.0) indicate a narrow molecular weight distribution and suggest that the extraction process preserved polymer uniformity, which is beneficial for consistent functional performance.

The ^{1}H-NMR spectrum of pectin in D_2O (600 MHz) exhibited characteristic resonances that confirmed the structural identity of the polysaccharide. Signals in the anomeric region at 4.90–5.10 ppm were attributed to H-1 protons of α-D-galacturonic acid units, while a distinct resonance at 4.40 ppm indicated the presence of neutral sugar residues such as galactose and arabinose. Strong peaks in the range of 3.72–3.90 ppm corresponded to $-OCH_3$ protons of methyl ester groups, whereas signals between 2.70–2.90 ppm reflected acetyl substituents ($-COCH_3$). Quantitative integration of methoxyl and anomeric proton signals enabled calculation of the degree of esterification (DE), revealing that the extracted pectin belongs to the high-methoxyl type (DE ~60%). This classification suggests strong gelling ability in the presence of sugar and acidic conditions. The coexistence of high and medium MW fractions, together with its high-methoxyl nature, indicates that this pectin may possess balanced functional properties, including stable film-forming ability, and strong gelling capacity. These features make coffee husk pectin a promising candidate for applications in food structuring and bio-based packaging materials.

3.3 Preparation of pectin-based roselle flower marmalade

3.3.1 Effect of heating time and temperature on the yield and color of roselle flower puree. Heat treatment is crucial in improving microbial safety and facilitating pectin solubilization from protopectin during cell wall degradation of roselle flower, thereby enhancing puree yield. Fig. 3 shows the effects of time and temperature on the yield and color of red roselle puree.

At 80 °C, puree yield was low (51.13% at 2 min) and decreased further with time (42.2% at 3 min and 38.01% at 4 min), indicating limited cell disruption and incomplete protopectin-to-pectin conversion (Fig. 3A). In contrast, at 85 °C and 90 °C, higher yields were observed due to enhanced thermal degradation of cell walls and denaturation of membrane proteins. The highest yield (67.72%) was recorded at 85 °C for 2 min but declined with longer heating (62.01% at 3 min; 53.66% at 4 min). At 90 °C, yield also decreased over time, from 63.76% (2 min) to 46.55% (4 min), likely due to irreversible damage to the protoplasmic membrane and excessive moisture loss. Maximum extractability occurred at 85 °C for 2 min, when protopectin was effectively solubilized into pectin, facilitating cell separation and juice release. Extended heating (4 min or more) reduced yield due to evaporation, nutrient degradation, and loss of structural integrity.

Temperature and time effect on enzyme inactivation which induce the change in color of the puree. At 80 °C for 2 min, color was brightest ($L^* = 56.72$, $a^* = 19.08$), with partial enzyme inactivation (Fig. 3B). However, incomplete enzyme inactivation could lead to pigment degradation during storage. At 85 °C for 2 min, color remained vibrant ($L^* = 53.32$, $a^* = 17.63$) due to effective inactivation of polyphenol oxidase (PPO) and peroxidase (POD), contributing to better pigment stability and microbial control. At 90 °C, anthocyanin degradation was accelerated, resulting in darker color ($L^* = 50.59$, $a^* = 15.48$ at 2 min; $L^* = 46.68$, $a^* = 10.29$ at 4 min). Thus, heating at 85 °C for 2 min was optimal, balancing enzyme inactivation, microbial safety, high puree yield, and preservation of color.

3.3.2 Influence of pectin on the textural properties of roselle marmalade. Pectin plays a pivotal role in determining

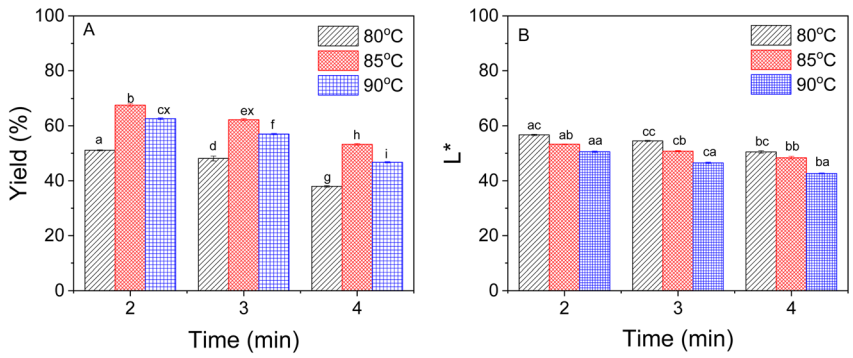

Fig. 3 Effect of heating time and temperature on yield (A) and color parameters (B) of red roselle puree. Different letters indicate statistically significant differences between samples ($P < 0.05$).

the gel strength and overall texture of marmalade, with both its botanical origin and concentration markedly impacting key mechanical attributes such as hardness and adhesiveness.[10] In this study, three pectin types, extracted from coffee husk, comercial lemon and orange peels, were investigated at a fixed concentration of 0.5% (w/w) to assess their effects on the texture of roselle marmalade (Fig. 4A). Among these, orange peel pectin resulted in the lowest gel hardness (7.23 N), which may be attributed to its relatively low DE. Pectins with lower DE values typically require higher sugar levels and acidic conditions to establish a stable gel matrix, and in low-sugar systems, such conditions may not suffice for optimal cross-linking. Consequently, this sample also exhibited the lowest adhesiveness (−2.54 N), likely due to limited methoxyl content and reduced intermolecular bonding capacity. Marmalade containing lemon peel pectin showed intermediate textural properties, with a hardness of 8.34 N and adhesiveness of −2.36 N. These improvements may be associated with its higher DE and methoxyl content, which promote more effective gelation through enhanced hydrogen bonding and hydrophobic interactions under acidic and sugary conditions.[37] Notably, coffee husk pectin demonstrated superior gelling capacity, yielding the highest hardness (10.08 N) and adhesiveness values. Its high DE may facilitate rapid gelation *via* junction zone formation, resulting in a denser and more cohesive polymer network that enhances resistance to deformation and improves overall textural integrity. This sample also exhibited increased adhesiveness, indicative of stronger molecular cohesion and reduced mobility among polymer chains.

To further explore the effect of pectin concentration, formulations using coffee husk pectin at varying levels (0.5–2.0%, w/w) were evaluated (Fig. 4). A significant positive correlation ($p < 0.05$) was observed between pectin concentration and hardness. The highest hardness (12.42 N) was recorded at 2.0% pectin, while the 0.5% formulation exhibited the lowest value (10.02 N). This trend aligns with the previous report indicating that an increase in pectin content enhances gel network density, thereby reinforcing structural rigidity.[53] Conversely, adhesiveness decreased as pectin concentration increased. This inverse relationship may be explained by the formation of a more stabilized gel matrix at higher pectin levels, which restricts polymer mobility and reduces tackiness at the gel surface.[54] Notably, at 0.5% coffee husk pectin, the marmalade exhibited balanced textural properties (hardness = 10.02 N; adhesiveness = −1.84 N), suggesting a favorable cross-linking density that maintains sufficient gel strength while preserving a soft, smooth, and spreadable consistency. This concentration appears optimal for delivering a desirable texture without over-hardening the product, making it suitable for consumer-preferred marmalade applications.

3.3.3 Influence of citric acid concentration on the acidity and color characteristics of roselle flower marmalade. Citric acid is commonly incorporated into fruit-based preserves to regulate pH and optimize gelation conditions. A suitable pH environment is essential for the effective gel-forming capability of pectin, as it promotes the formation of junction zones and stabilizes the gel network.[54] Additionally, low pH conditions contribute to microbial inhibition, particularly of spoilage organisms such as *Aspergillus* and *Penicillium* species, thereby enhancing the microbial safety and shelf stability of marmalade products. Beyond its acidifying role, citric acid also prevents sucrose crystallization during storage, ensuring a smooth texture and preventing undesirable syneresis or sugar recrystallization in the marmalade.

However, the concentration of citric acid must be carefully optimized, as excessive amounts may adversely impact the organoleptic and visual attributes of the marmalade. Fig. S4 showed that at a low concentration of 0.5%, the marmalade exhibited a total acidity (TA) of 0.28%, a pH of 3.5, and a lightness (L^*) value of 55.14. These values were insufficient to elicit a pronounced acidic taste and were associated with a relatively darker color tone, likely due to limited inhibition of enzymatic browning and pigment degradation. In contrast, higher citric acid concentrations (1.5–2.0%) increased the TA to 0.51–0.60% and reduced the pH to 3.3–3.2, with corresponding L^* values of 48.60 and 36.80, respectively. Although these samples exhibited lighter coloration due to more effective inhibition of enzymatic oxidation and pigment breakdown, the intense sourness rendered the product less palatable for general consumption.

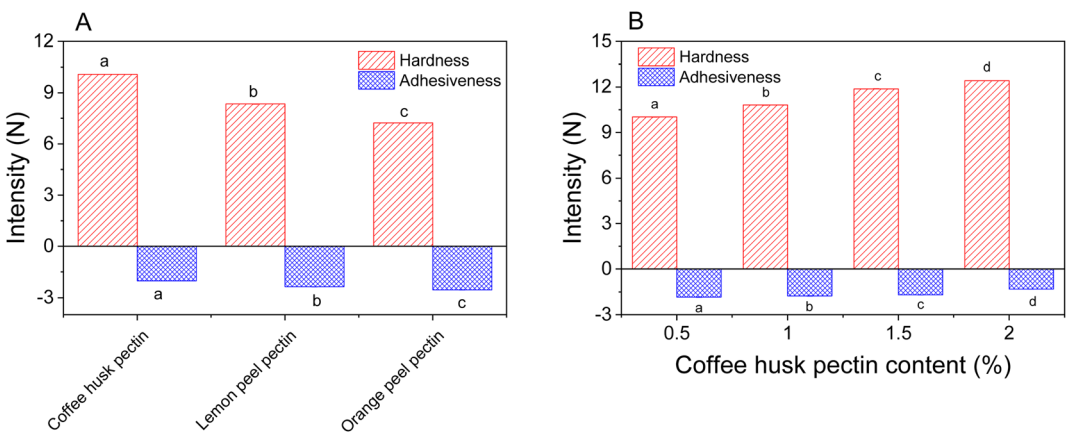

Fig. 4 Influence of different pectin types (A) and coffee husk pectin content (B) on the textural properties of roselle flower marmalade. Distinct letters indicate statistically significant differences between samples ($P < 0.05$).

The marmalade formulated with 1.0% citric acid achieved a favorable balance, exhibiting a TA of 0.35%, pH of 3.4, and L^* value of 50.28. This concentration provided a moderate yet perceptible acidity, contributing to flavor enhancement without overpowering sourness. Moreover, the pH level in this formulation remained below the critical threshold for microbial growth (pH < 4.5), offering protection against spoilage microorganisms. Simultaneously, it contributed to improved pigment stability by reducing enzymatic oxidation reactions, thereby preserving a bright and appealing red hue in the final product. Based on these results, the 1.0% citric acid concentration was selected as the optimal level for developing coffee husk pectin-based roselle marmalade, as it ensured a desirable balance between acidity, microbial stability, and color retention.

3.3.4 Effect of sucrose concentration on color attributes and sensory properties of pectin-based roselle flower marmalade. Sucrose concentration plays a critical role in modulating the color, texture, and overall quality of pectin-based roselle flower marmalade. In this study, formulations were prepared with varying sucrose levels (40–55%, w/w) and concentrated until a final soluble solids content of 65° Brix was achieved. The color parameters (L^*, a^*, b^*) of the resulting marmalades are shown in Fig. 5. At lower sucrose levels (40% and 45%), the marmalades displayed significantly darker coloration, with L^* values of 40.62 and 43.83, respectively. This can be attributed to prolonged heating times required to reach the target Brix level, which intensifies non-enzymatic browning reactions and degradation of thermolabile pigments such as anthocyanins and polyphenols, resulting in a darker appearance and potential color loss.

Conversely, the sample with the highest sucrose content (55%) had a comparatively lighter color ($L^* = 46.61$), due to the shorter heating time required to achieve 65° Brix. However, the elevated sugar level may have promoted excessive caramelization during concentration, leading to an undesirable burnt flavor and off-color formation. Notably, the formulation containing 50% sucrose exhibited the highest L^* value (49.69), along with optimal a^* and b^* values (11.09 and 5.09, respectively), indicating a bright and appealing reddish hue. This outcome suggests that at this sucrose concentration, the heating time was sufficiently balanced, minimizing pigment degradation while allowing controlled caramelization to develop flavor and enhance color without charring.

To assess consumer acceptance, sensory evaluation was conducted following a three-day storage period. Twelve semi-trained panelists were recruited, and each participant received randomized coded samples along with standardized evaluation instructions.[55] According to ANOVA results, significant differences ($P < 0.05$) were observed in sensory attributes across samples with varying sucrose concentrations. The 50% sucrose sample consistently received the highest hedonic ratings across all categories. Specifically, it scored 3.5 ± 0.38 for aroma, 4.5 ± 0.00 for taste, 4.5 ± 0.02 for color, 4.4 ± 0.38 for texture acceptability.

In terms of flavor, samples with 40–50% sucrose showed statistically significant differences ($P < 0.05$), while the 55% sample did not significantly differ from the 50% formulation. Although the 55% sample achieved acceptable sweetness, the overdeveloped caramel notes and potential color distortion may have negatively impacted its overall perception. The 50% sucrose sample was characterized by a well-balanced sweetness, vibrant color, desirable gel consistency, and a distinctive roselle aroma, which collectively contributed to its highest overall acceptability score ($P = 0.015 < 0.05$). These findings suggest that 50% sucrose represents the optimal concentration for formulating roselle marmalade, achieving a harmonious balance between visual appeal, flavor intensity, textural integrity, and consumer preference.

3.4 Composite of coffee husk pectin/chitosan for fruit coating

3.4.1 Physicochemical properties of coffee husk pectin/chitosan composites. Swelling ratio (SR), water solubility (WS), and water vapor permeability (WVP) are critical indicators of the hydrophilicity and water resistance of biofilms, and thus play a decisive role in their suitability as packaging materials for fresh fruits with high moisture content. As shown in Fig. 6A, the CP film exhibited higher SR and WVP values compared to CPC and CPP films. This can be attributed to the formation of a denser polymeric network through strong intermolecular interactions between pectin and chitosan, together with the

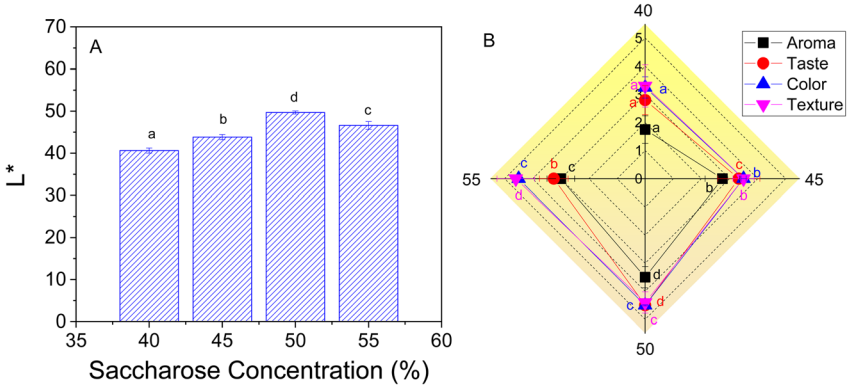

Fig. 5 Effect of saccharose concentration on color parameter (A) and sensory (B) obtained from 20 volunteer panelists. Distinct letters indicate statistically significant differences between samples ($P < 0.05$).

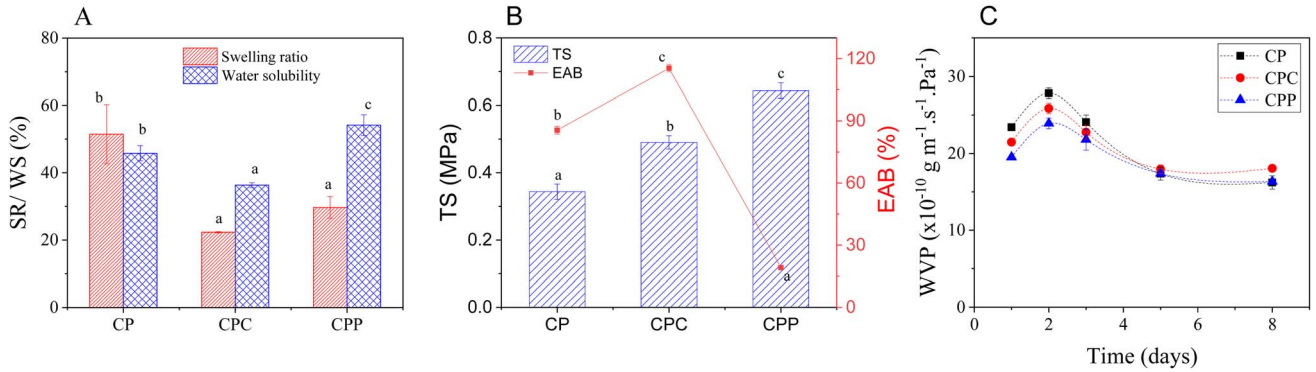

Fig. 6 Swelling ratio, and water solubility (A); tensile strength (TS) and elongation at break (EAB) (B); and water vapor permeability *versus* time (C) of the various biofilms: chitosan/pectin (CP); chitosan/pectin/curcumin (CPC); chitosan/pectin/pormergranate peel extract (CPP).

cross-linking effects of bioactive compounds. In general, SR reflects the water absorption capacity of films, while WS indicates the extent of dissolution in aqueous environments, and these two parameters are often positively correlated. However, the results reveal a distinct trend among the CP, CPC, and CPP films. Specifically, CPC films containing curcumin displayed reduced WS due to the hydrophobicity of curcumin, despite their ability to absorb water. In contrast, CPP films exhibited both high SR and unexpectedly higher WS, which can be ascribed to the abundant hydrophilic hydroxyl and carboxyl groups of polyphenolic compounds from pomegranate peel extract. These groups facilitate water penetration and polymer dissolution, thereby explaining the apparent divergence from the expected SR–WS correlation.

The tensile strength (TS) and elongation at break (EAB) of the biofilms are illustrated in Fig. 6B. Significant variations were observed among the formulations, reflecting the different roles of curcumin and pomegranate peel extract in modulating the polymeric network. The pristine CP film exhibited the lowest TS (0.34 ± 0.02 MPa), indicating weak intermolecular interactions between pectin and chitosan. Upon incorporation of curcumin, the TS value markedly increased to 0.49 ± 0.02 MPa. This enhancement can be ascribed to the ability of curcumin molecules to establish hydrogen bonding and hydrophobic interactions with both polysaccharides, thereby reinforcing the polymeric matrix. More pronounced reinforcement was achieved with the addition of pomegranate peel extract, yielding the highest TS (0.64 ± 0.02 MPa). This result suggests that the abundant polyphenolic constituents in pomegranate peel, such as tannins and flavonoids, promote extensive hydrogen bonding and potential π–π stacking interactions, leading to a more compact and rigid network structure.

In contrast, the EAB values exhibited an opposite trend. The CP film displayed a moderate flexibility ($85.5 \pm 1.9\%$), which further improved in the CPC film ($115.3 \pm 1.8\%$). The enhanced ductility of CPC could be attributed to curcumin acting as a natural plasticizer, increasing chain mobility and preventing excessive aggregation of the biopolymers. Conversely, the CPP film demonstrated a sharp decrease in EAB ($19.1 \pm 0.85\%$), indicating brittle behavior. This reduction is likely due to the strong crosslinking effects of polyphenols that restrict chain mobility, thereby enhancing stiffness at the expense of flexibility.

Additionally, the WVP of all films decreased significantly over time compared to their initial values. This reduction may be due to water vapor filling the microvoids within the film structure, leading to a denser and more compact matrix that limits both water absorption and vapor transmission.

The physicochemical and morphological properties of the prepared films were systematically investigated using X-ray diffraction (XRD), fourier-transform infrared spectroscopy (FTIR), thermogravimetric analysis (TGA), and scanning electron microscopy (SEM), as shown in Fig. 7.

The XRD patterns of pectin, CP, CPC, and CPP are presented in Fig. 7A. All samples exhibit broad, diffuse bands centered at 2θ of 22.7°, indicating their predominantly amorphous structure. Pure pectin shows a typical amorphous pattern, while the CP film retains this behavior with slight broadening and shifting of the peak (22.7°), suggesting intermolecular hydrogen bonding between chitosan and pectin chains. Notably, the addition of curcumin or pomegranate extract does not introduce any crystalline peaks, implying that these bioactives are either molecularly dispersed or present in a non-crystalline state within the polymer matrix. The results confirm that all formulations are structurally amorphous, with good miscibility between components and no evidence of phase separation or crystallization.

Fig. 7B displays the FTIR spectra of the CP, CPC, and CPP films. All samples exhibit a broad absorption band centered at 3420 cm^{-1}, which corresponds to the stretching vibrations of O–H and N–H groups. This broad band is indicative of an extensive hydrogen-bonding network among the hydroxyl and amino groups present in both polysaccharide chains and incorporated bioactive compounds. A distinct peak at 1728 cm^{-1} is assigned to the C=O stretching vibration of esterified carboxyl groups in pectin, while the band at 1624 cm^{-1} is attributed to the asymmetric stretching of carboxylate anions (COO^-) in pectin and the amide I band of chitosan. The intensity ratio between the 1624 cm^{-1} and 1728 cm^{-1} bands is markedly higher in the CP film compared to

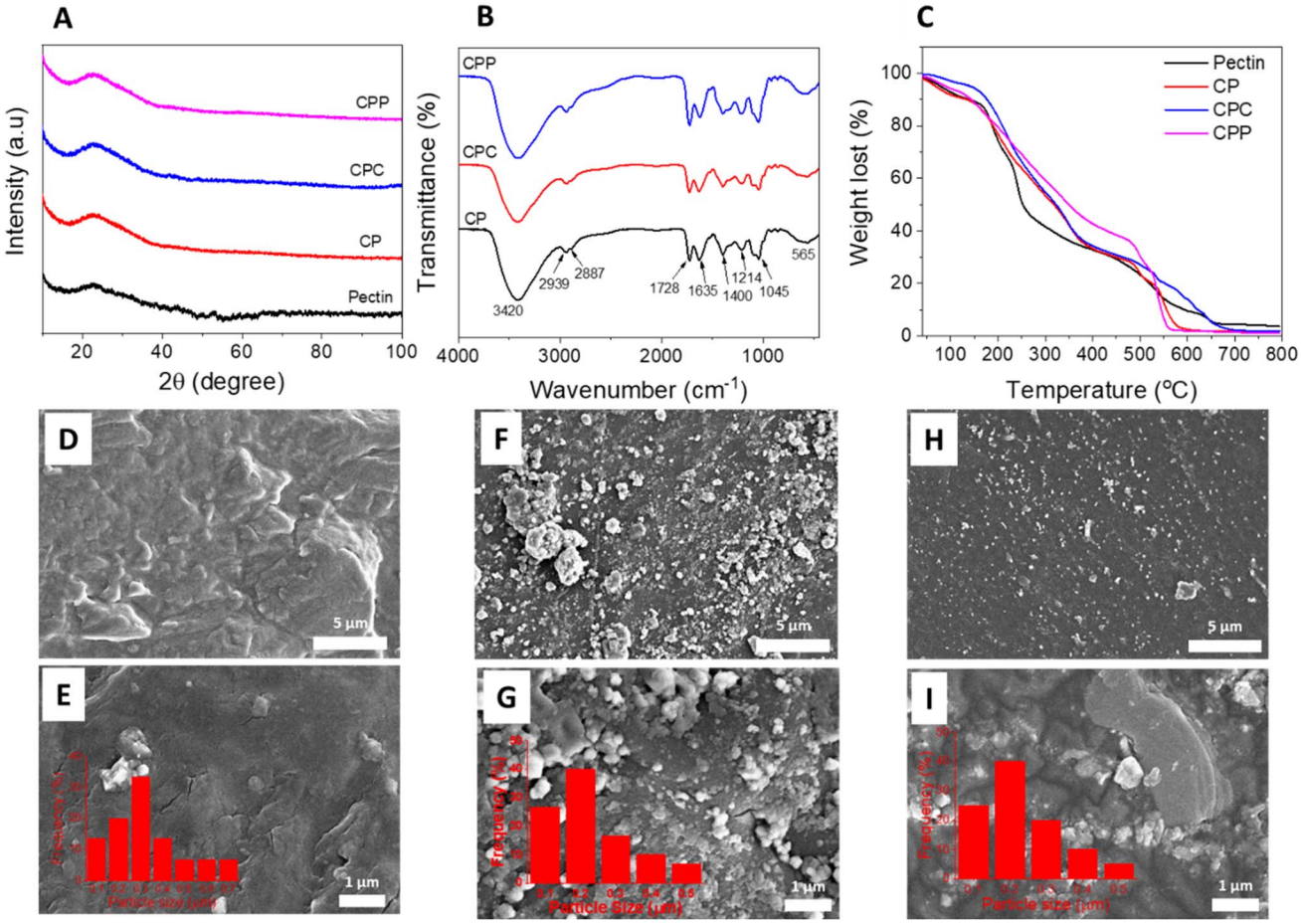

Fig. 7 (A) X-ray diffraction (XRD) patterns, (B) Fourier-transform infrared (FTIR) spectra, and (C) thermogravimetric analysis (TGA) curves of pectin, chitosan/pectin (CP), chitosan/pectin/curcumin (CPC), and chitosan/pectin/pomegranate (CPP) samples. SEM images and particle size distribution (inset) of CP (D and E), CPC (F and G) and CPP (H and I) at different magnifications (bar = 5 μm and 1 μm).

that of pure pectin (Fig. S1B), confirming the presence of chitosan in the film matrix. Interestingly, this ratio slightly decreases in the CPC and CPP films, which can be attributed to the additional C=O functional groups introduced by curcumin and bioactive compounds present in the pomegranate extract. These overlapping signals contribute to the overall intensity of the 1728 cm^{-1} band, thus lowering the relative ratio. Collectively, these spectral changes provide strong evidence of successful incorporation of curcumin and pomegranate extract into the CP network, likely through non-covalent interactions such as hydrogen bonding, electrostatic attraction, or hydrophobic association.

The thermal stability of the films was investigated using thermogravimetric analysis (TGA), and the results are shown in Fig. 7C. Pure pectin exhibited a typical three-step degradation profile: an initial weight loss (~10%) below 150 °C due to evaporation of physically adsorbed and bound water; major decomposition between 200–250 °C related to depolymerization and cleavage of glycosidic linkages (≈40% weight loss); and complete degradation up to 600 °C, leaving minimal residue. In comparison, the CP film showed improved thermal stability, with only ~30% weight loss at 250 °C. This enhancement is attributed to intermolecular hydrogen bonding between chitosan and pectin, which reinforces the polymer network and delays thermal degradation. The CPC film exhibited a similar degradation pattern to CP up to 500 °C but demonstrated higher resistance at elevated temperatures, with complete decomposition occurring closer to 700 °C. This extended stability likely arises from curcumin–polymer interactions that suppress chain scission and promote char formation. The CPP film also showed improved stability below 500 °C compared to CP and neat pectin, confirming reinforcement by pomegranate-derived polyphenols. However, its stability beyond 500 °C was slightly lower than CPC, reflecting the heterogeneous nature of the extract and its less uniform interactions within the matrix. Residual mass at 600 °C followed the order CPP > CPC ≈ CP > pectin.

From a practical perspective, these results indicate that all composite films (CP, CPC, and CPP) maintain structural stability well above 100 °C, far exceeding typical storage and handling conditions for food products (room temperature to ≤ 60 °C). The incorporation of curcumin and pomegranate extract further enhanced thermal resistance, suggesting that these films are unlikely to undergo degradation or loss of integrity

during real storage, transportation, or moderate processing operations such as pasteurization. Therefore, the improved thermal stability not only supports material robustness but also enhances their suitability as bio-based packaging films for practical food preservation.

The surface morphology of the films was examined using scanning electron microscopy (SEM), as illustrated in Fig. 7D–I. The CP film (Fig. 7D and E) exhibited a dense, and continuous surface without visible phase separation. This homogeneity indicates excellent miscibility between chitosan and pectin, and reflects the formation of a cohesive biopolymer matrix with uniform structural integrity. In contrast, the CPC film (Fig. 7F and G) displayed a rougher surface texture, along with the presence of small particulate domains or micro-aggregates, which may be associated with the localized distribution of curcumin within the matrix. These morphological features suggest that curcumin interacts non-uniformly with the polymer chains, potentially forming hydrogen-bonded clusters or semi-separated microphases. The CPP film (Fig. 7H and I) exhibited an irregular, grainy, and slightly porous morphology, which is likely due to the chemical complexity and heterogeneous composition of the pomegranate extract. Polyphenolic compounds, organic acids, and sugars present in the extract may interact differentially with the chitosan–pectin matrix, resulting in less compact packing and uneven surface features. Despite this, no delamination was observed, indicating that the film structure remains intact and processable. The observed morphological differences confirm that the addition of curcumin or pomegranate extract modifies surface characteristics without compromising film cohesion. These structural features, particularly the homogeneity and flexibility of CP, CPC, and CPP support the potential application of these films as biodegradable and functional materials for fruit packaging.

The particle size distribution obtained from SEM analysis provided additional insight into the microstructural characteristics of the films. Although the CP film exhibited a smoother surface compared to CPC and CPP, it contained relatively larger particles, with the majority concentrated in the 0.2–0.3 μm range. In contrast, the CPC film showed a higher frequency of smaller particles (0.1–0.2 μm) and the highest particle density among the three samples, reflecting the presence of micro-aggregates and confirming that curcumin was not uniformly dispersed but instead formed localized clusters. The CPP film also displayed a narrow distribution within the 0.1–0.2 μm range; however, its particle density was considerably lower. This result is consistent with the chemical complexity of pomegranate peel extract, which likely induced heterogeneous interactions with the chitosan–pectin matrix, leading to less compact packing and the formation of more porous surface features.

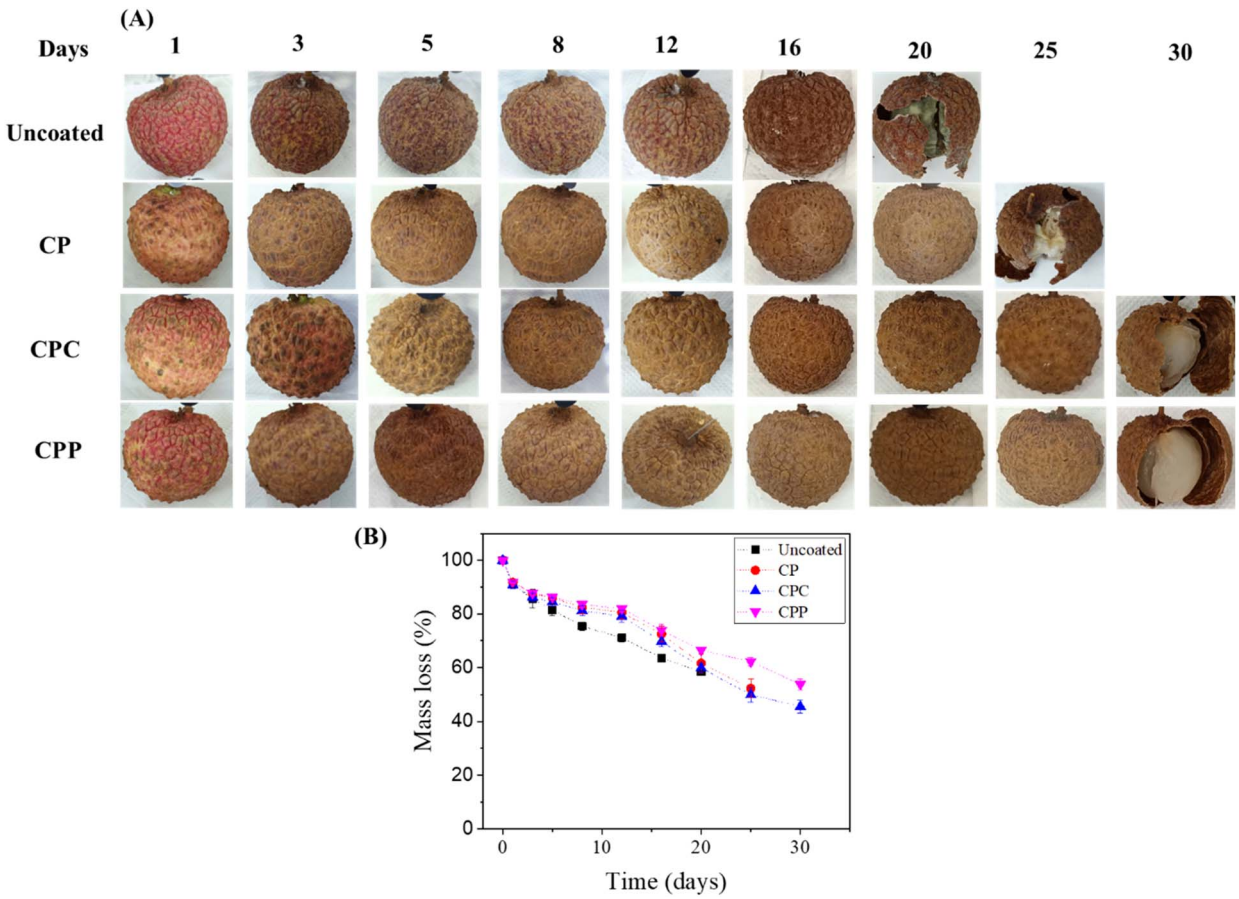

Fig. 8 The photos of lychee (*Litchi chinensis*) coated (A) and plots of mass loss *versus* storage time of litchi (B): blank, CP, CPC, and CPP biofilms.

3.4.2 Antioxidant activity. The incorporation of natural antioxidants into biopolymer films is a widely explored strategy for developing active food packaging systems. In this study, curcumin (CPC) and pomegranate peel extract (CPP) were introduced into CP film to enhance their antioxidant properties, as evaluated by DPPH and hydrogen peroxide (H_2O_2) scavenging assays. As shown in Table S2, the control CP film exhibited moderate antioxidant activity with a DPPH scavenging efficiency of 33.86 ± 2.18% and H_2O_2 scavenging of 20.48 ± 0.93%. The incorporation of CPC significantly increased these values to 49.04 ± 1.08% and 31.91 ± 1.32%, respectively, while CPP showed the highest enhancement, reaching 64.55 ± 1.80% for DPPH and 48.08 ± 2.11% for H_2O_2 scavenging. These results confirm that both curcumin and pomegranate peel extract significantly improve the radical scavenging capacity of the films ($p < 0.05$), consistent with their known phenolic and flavonoid content.[56,57]

These findings suggest that the antioxidant-enhanced films have strong potential for retarding oxidative spoilage in lipid-containing foods. By reducing free radical activity and peroxide formation, the active films may contribute to preserving nutritional quality, delaying rancidity, and extending shelf life during storage.

3.4.3 Fruit coating. The application of CP-based films, including those incorporated with curcumin (CPC) and pomegranate peel extract (CPP), demonstrated a pronounced effect on the postharvest preservation of *Litchi chinensis* fruits (Fig. 8). Compared to the uncoated control group, the coated samples exhibited significantly lower weight loss during storage. After 12 days at ambient conditions, the coated fruits retained approximately 80% of their initial weight, whereas the control fruits maintained only ~70%, highlighting the efficacy of the bioactive films in reducing moisture loss and delaying senescence.

Beyond weight retention, the coatings also played a critical role in inhibiting microbial and fungal growth. In the control samples, visible white mold developed both on the fruit surface and within the pulp by day 16, rendering them unmarketable. In contrast, fruits coated with the CP film showed delayed fungal growth, with no visible spoilage until day 25. Even after 20 days of storage, CP-coated fruits retained ~65% of their original weight and exhibited minimal signs of deterioration. Notably, the incorporation of antioxidant and antimicrobial agents such as curcumin and pomegranate peel extract substantially enhanced the protective effect. The CPC- and CPP-coated lychees exhibited no internal fungal contamination throughout the 30 days storage period. By day 30, fruits treated with CPC and CPP films retained 45.5 ± 2.4% and 53.8 ± 2.1% of their initial weight, respectively, while maintaining fresh aroma, acceptable texture, and no visible fungal growth. These results suggest that curcumin and pomegranate peel extract not only act as antioxidants but also contribute antifungal activity, synergistically extending the shelf life and preserving the overall

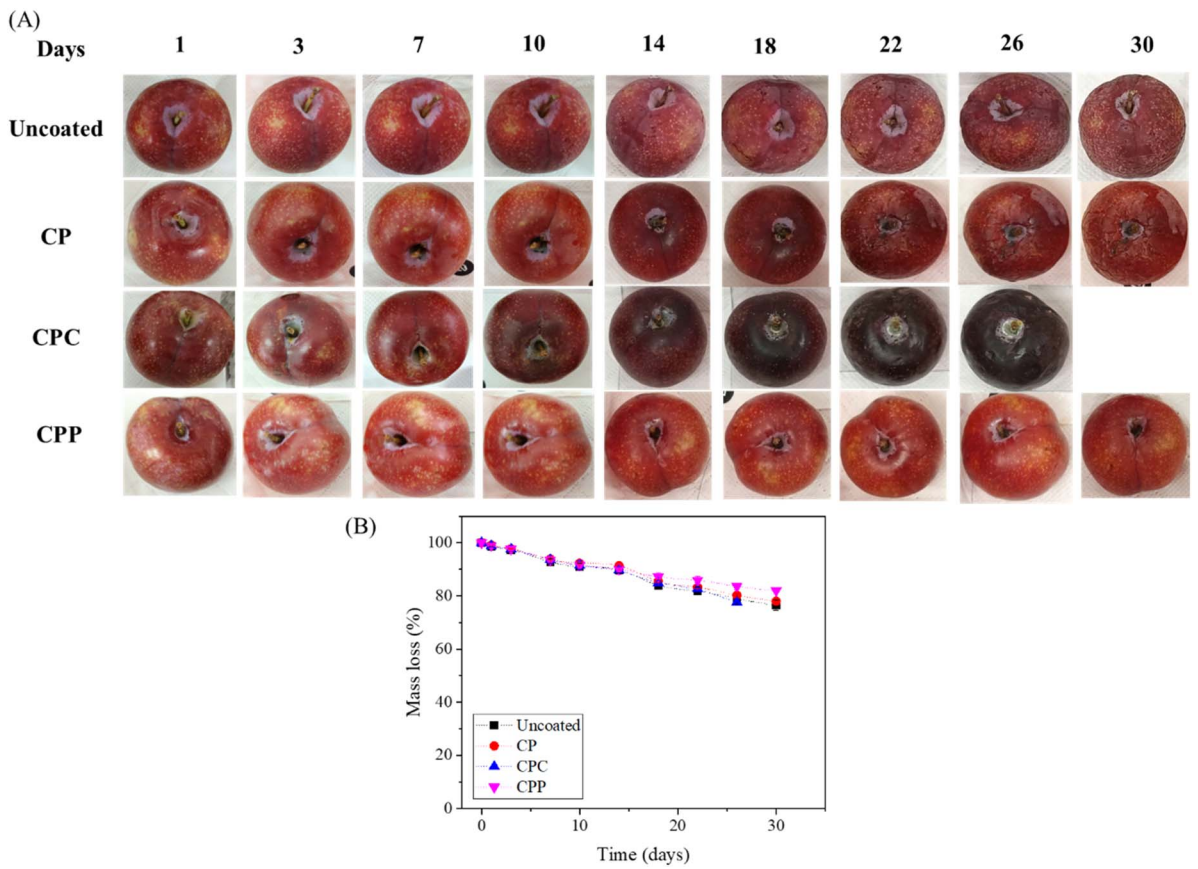

Fig. 9 The photos of Japanese plum (*Prunus salicina*) coated (A) and plots of mass loss *versus* storage time of litchi (B): blank, CP, CPC, and CPP biofilms.

quality of lychee fruits under non-refrigerated conditions. These findings align with the previous study reporting the efficacy of bioactive coatings in reducing postharvest losses through moisture barrier properties and antimicrobial actions.[58] The dual function of these coatings, retarding weight loss and inhibiting spoilage, underscores their potential for sustainable and natural postharvest preservation strategies in the fresh produce industry.

The postharvest performance of bioactive coatings was further evaluated on Japanese plum (*Prunus salicina*) to assess their applicability across different fruit matrices. A storage experiment was conducted under the same conditions as for lychee, employing periodic external observation and measurement of weight loss to monitor changes in fruit quality throughout the storage period (Fig. 9).

During the first 18 days, there were no statistically significant differences in weight loss among the coated (CP, CPC, CPP) and uncoated control groups. All samples exhibited minimal dehydration and retained similar external appearance. However, starting from day 20, visible signs of quality degradation became apparent in the control and CP- and CPC-coated groups, including surface wrinkling and loss of firmness, symptoms commonly associated with progressive moisture loss and senescence in plums. Notably, by day 26, the fruits coated with CPC films exhibited pronounced softening and developed a darker reddish-purple hue. This accelerated ripening and discoloration may be attributed to the interaction between curcumin and phenolic compounds naturally present on the plum surface, potentially catalyzing anthocyanin transformation or promoting enzymatic browning. These observations align with reports on pro-oxidant or pigment-modulating behavior of curcumin under certain conditions.[59,60]

At the end of the 30 days storage period, quantitative weight loss measurements revealed that the uncoated fruits retained 76.4 $\pm$ 1.9% of their initial weight, while those coated with CP and CPP films retained 77.9 $\pm$ 0.9% and 81.9 $\pm$ 0.7%, respectively. Although the differences in weight retention among coated groups were moderate, the CPP-coated fruits displayed superior visual and textural quality. They maintained smooth skin, minimal surface wrinkling, and firm flesh without signs of over-ripening or fungal decay. In contrast, CP- and CPC-coated samples exhibited varying degrees of softening, skin dullness, and color changes, which can negatively impact marketability. These findings suggest that while CP-based coatings are generally beneficial for delaying postharvest deterioration in *Prunus salicina*, the incorporation of pomegranate peel extract (CPP) offers additional advantages in preserving fruit firmness, preventing skin wrinkling, and maintaining overall freshness during extended storage.

The results highlight the selective effectiveness of natural additives, depending on fruit type and physiology, and reinforce the importance of tailoring coating formulations for specific produce.

4. Conclusion

Waste robusta coffee husk was successfully valorized as a novel pectin source through ultrasound-assisted extraction, achieving a high yield of 16.4%. The extracted pectin exhibited suitable gelling properties, enabling its application in roselle marmalade. Formulations containing 0.5% coffee husk pectin, 1.0% citric acid, and 50% sucrose produced marmalade with favorable texture and sensory acceptability, confirming its functionality as a citrus pectin alternative. When incorporated into chitosan-based biofilms, the pectin contributed to enhanced barrier and mechanical properties. The addition of natural antioxidants, curcumin (CPC) and pomegranate peel extract (CPP), significantly improved radical scavenging activity. Postharvest application of these films demonstrated strong protective effects. Lychee fruits coated with CPP film retained 53.8 $\pm$ 2.1% of their original weight after 30 days of storage at ambient conditions, with no visible fungal growth, compared to only 45.5 $\pm$ 2.4% for CPC while uncoated samples were decomposed completely after only 20 days. In Japanese plums, CPP coatings maintained 81.9 $\pm$ 0.7% weight retention, preserved skin smoothness, and prevented over-ripening more effectively than other treatments. These findings confirm the dual functionality of coffee husk pectin in food and active packaging applications, supporting sustainable material innovation and circular bioeconomy goals.

Author contributions

Thi-Ngoc-Mai Tran: investigation, formal analysis, validation, software, originate manuscript; Nguyen-Trung-Tien Dieu, Thi-Hong-No Nguyen, Van-Dung Le, Chi-Hien Dang: investigation, visualization, validation; Dinh-Tri Mai, Thanh-Danh Nguyen: conceptualization, supervisor, writing – review & editing.

Conflicts of interest

The authors of this paper state that they have no competing financial interests or personal relationships that could have influenced the reported work.

Data availability

The data supporting this article have been included as part of the supplementary information (SI). Supplementary information is available. See DOI: **https://doi.org/10.1039/d5ra05086c**.

Acknowledgements

This research is funded by Vietnam Academy of Science and Technology under grant number NCXS02.04/24–25.

References

1 N. M. Rotta, S. Curry, J. Han, R. Reconco, E. Spang, W. Ristenpart and I. R. Donis-González, *Resour., Conserv. Recycl.*, 2021, **170**, 105554.
2 S. B. Magar, B. Thagunna, B. Lamichhane, B. Pokhrel and J. Kaur, *Int. J. Food Ferment. Technol.*, 2023, **13**, 87–94.
3 L. S. Oliveira and A. S. Franca, *Coffee in Health and Disease Prevention*, 2015, pp. 283–291.

4 K. Tamilselvan, S. Sundarajan, S. Ramakrishna, A.-A. A. Amirul and S. Vigneswari, *Food Bioprod. Process.*, 2024, **145**, 187–202.
5 K. Tsigkou, B. A. Demissie, S. Hashim, P. Ghofrani-Isfahani, R. Thomas, K. F. Mapinga, S. K. Kassahun and I. Angelidaki, *Renewable Sustainable Energy Rev.*, 2025, **210**, 115263.
6 K. Tamilselvan, S. Sundarajan, S. Ramakrishna, A.-A. A. Amirul and S. Vigneswari, *Food Bioprod. Process.*, 2024, **145**, 187–202.
7 H. Chanakya and A. De Alwis, *Process Saf. Environ. Prot.*, 2004, **82**, 291–300.
8 Z. Li, B. Zhou, T. Zheng, C. Zhao, Y. Gao, W. Wu, Y. Fan, X. Wang, M. Qiu and J. Fan, *Foods*, 2023, **12**, 423.
9 G. Divyashri, T. P. K. Murthy, K. V. Ragavan, G. M. Sumukh, L. S. Sudha, S. Nishka, G. Himanshi, N. Misriya, B. Sharada and R. A. Venkataramanaiah, *Heliyon*, 2023, **9**, e20212.
10 D. Gawkowska, J. Cybulska and A. Zdunek, *Polymers*, 2018, **10**, 762.
11 S. M. Haque, A. Kabir, E. Ratemi, M. Elzagheid, S. P. Appu, S. S. Ghani and A. Sarief, *Separations*, 2025, **12**, 65.
12 R. Malpartida Yapias, F. Ore Areche, J. Echevarria Victorio, J. Paucarchuco Soto, G. Lobato Calderon, E. Palomino Santos, J. Montalvo Otivo, C. Flores-Miranda and A. Ruiz Rodriguez, *Braz. J. Microbiol.*, 2025, **85**, e287792.
13 K. Kumar, S. Srivastav and V. S. Sharanagat, *Ultrason. Sonochem.*, 2021, **70**, 105325.
14 K. M. Wani and R. V. Uppaluri, *Biomass Convers. Biorefin.*, 2024, **14**, 28603–28618.
15 V. Shruthi and C. Ramachandra, in *Food bioactives*, Apple Academic Press, 2019, pp. 169–190.
16 N. L. Mohammed Yusof, S. Zainalabidin, N. Mohd Fauzi and S. B. Budin, *Appl. Physiol., Nutr., Metab.*, 2018, **43**, 1224–1232.
17 F. H. AL-Jawad, H. Hashim, Z. Al-Attar and A. H. Al-Ani, *World. J. Pharm. Sci.*, 2018, **4**, 125–134.
18 B. W. Hapsari and W. Setyaningsih, *Horticulturae*, 2021, **7**, 35.
19 P. Ochelle, S. Torkuma and P. Swande, *Applied Sciences Research Periodicals*, 2024, **2**, 74–95.
20 A. Arslaner, M. A. Salik and I. Bakirci, *J. Taiwan Inst. Chem. Eng.*, 2021, **58**, 223–233.
21 V. Sicari, T. M. Pellicanò, V. Laganà and M. Poiana, *J. Food Process. Preserv.*, 2018, **42**, e13429.
22 E. Scarcelli, A. Catalano, D. Iacopetta, J. Ceramella, M. S. Sinicropi and F. Aiello, *Macromol*, 2025, **5**, 15.
23 O. Phonrachom, P. Charoensuk, K. Kiti, N. Saichana, P. Kakumyan and O. Suwantong, *Int. J. Biol. Macromol.*, 2023, **241**, 124633.
24 P. D. Hoagland and N. Parris, *J. Agric. Food Chem.*, 1996, **44**, 1915–1919.
25 R. Kumar and A. K. Rai, *World J. Pharm. Res.*, 2017, **6**, 1501–1530.
26 J. Jovanović, J. Ćirković, A. Radojković, D. Mutavdžić, G. Tanasijević, K. Joksimović, G. Bakić, G. Branković and Z. Branković, *Prog. Org. Coat.*, 2021, **158**, 106349.
27 B. R. Machado, S. P. Facchi, A. C. de Oliveira, C. S. Nunes, P. R. Souza, B. H. Vilsinski, K. C. Popat, M. J. Kipper, E. C. Muniz and A. F. Martins, *Int. J. Mol. Sci.*, 2020, **21**, 8663.
28 N. Aliabbasi, M. Fathi and Z. Emam-Djomeh, *J. Environ. Chem. Eng.*, 2021, **9**, 105520.
29 X. Qu, X. Wang, W. Guan, Y. Zhao and J. Li, *Food Bioprocess Technol.*, 2024, **17**, 2973–2997.
30 Z. N. Hanani, F. C. Yee and M. Nor-Khaizura, *Food Hydrocolloids*, 2019, **89**, 253–259.
31 H. Li, Y. Jiang, J. Yang, R. Pang, Y. Chen, L. Mo, Q. Jiang and Z. Qin, *Food Hydrocolloids*, 2023, **145**, 109150.
32 S. F. Mirpoor, S. M. H. Hosseini and G. H. Yousefi, *Food Hydrocolloids*, 2017, **71**, 216–224.
33 H. Cui, D. Surendhiran, C. Li and L. Lin, *Food Packag. Shelf Life*, 2020, **24**, 100511.
34 T. Kaseke, S. C. Chew, T. P. Magangana and O. A. Fawole, *Food Bioprocess Technol.*, 2025, **18**, 4222–4250.
35 L. H. Reichembach and C. L. de Oliveira Petkowicz, *Carbohydr. Polym.*, 2020, **245**, 116473.
36 R. L. Azzahra, P. Lestari, D. Y. Susanti, N. C. Dione and A. M. Chairani, Preparation and Extraction of Pectin from Robusta Coffee (Coffea canephora) Peel Waste as a Sustainable Agriculture Biomass, in *Proceedings of the BIO Web of Conferences*, 2025, p. 09001.
37 P. Skenderidis, S. Leontopoulos, K. Petrotos and I. Giavasis, *Foods*, 2020, **9**, 1655.
38 J. López-Mercado, A. Nambo, M.-E. Toribio-Nava, O. Melgoza-Sevilla, L. Cázarez-Barragán, L. Cajero-Zul, L.-G. Guerrero-Ramírez, B. E. Handy and M.-G. Cardenas-Galindo, *Clean Technol. Environ. Policy*, 2018, **20**, 1413–1422.
39 R. Zhi, L. Zhao and J. Shi, *J. Dairy Sci.*, 2016, **99**, 5305–5317.
40 J. Yan, R. Cui, Y. Qin, L. Li and M. Yuan, *Int. J. Biol. Macromol.*, 2021, **177**, 328–336.
41 T. T. T. Nguyen, T. Q. Le, T. T. A. Nguyen, L. T. M. Nguyen, D. T. C. Nguyen and T. Van Tran, *Heliyon*, 2022, **8**(8), e10096.
42 K. Zhang, T.-S. Huang, H. Yan, X. Hu and T. Ren, *Int. J. Biol. Macromol.*, 2020, **145**, 768–776.
43 Y.-T. Kim, R. Kimmel and X. Wang, *Molecules*, 2023, **28**, 2092.
44 D. Mukhopadhyay, P. Dasgupta, D. S. Roy, S. Palchoudhuri, I. Chatterjee, S. Ali and S. G. Dastidar, *Free Radicals and Antioxidants*, 2016, 6, pp. 124–132.
45 K. Tarangini, P. Kavi and K. Jagajjanani Rao, *eFood*, 2022, **3**, e36.
46 O. A. Fakayode and K. E. Abobi, *J. Anal. Sci. Technol.*, 2018, **9**, 1–16.
47 F. Dranca and M. Oroian, *Processes*, 2019, **7**, 488.
48 L. Shen, S. Pang, M. Zhong, Y. Sun, A. Qayum, Y. Liu, A. Rashid, B. Xu, Q. Liang and H. Ma, *Ultrason. Sonochem.*, 2023, **101**, 106646.
49 K. Peng, F. G. Qin, R. Jiang and S. Kang, *Ultrason. Sonochem.*, 2020, **69**, 105253.
50 F. Luo, Z. Zhang, F. Lu, D. Li, C. Zhou, Y. Li, L. Niu, Y. Xu, L. Feng and Z. Dai, *Food Hydrocolloids*, 2024, **152**, 109898.
51 A. Forouhar, N. Hamdami, G. Djelveh, C. Gardarin, G. Pierre, A. V. Ursu and P. Michaud, *Appl. Sci.*, 2023, **13**, 5558.
52 C. G. Nadar, A. Arora and Y. Shastri, *ACS Eng. Au*, 2022, **2**, 61–74.
53 Y. Kakino, Y. Hishikawa, R. Onodera, K. Tahara and H. Takeuchi, *Chem. Pharm. Bull.*, 2017, **65**, 1035–1044.

54 N. S. Said, I. F. Olawuyi and W. Y. Lee, *Gels*, 2023, **9**, 732.
55 S. Park, J. Heo, J. Oh, S.-J. Chung and H. S. Kwak, *Food Qual. Prefer.*, 2023, **109**, 104905.
56 N. Kumar, Pratibha, A. Trajkovska Petkoska, E. Khojah, R. Sami and A. A. Al-Mushhin, *Materials*, 2021, **14**, 3305.
57 M. Cvek, U. C. Paul, J. Zia, G. Mancini, V. Sedlarik and A. Athanassiou, *ACS Appl. Mater. Interfaces*, 2022, **14**, 14654–14667.
58 N. Kumar, Neeraj, Pratibha and M. Singla, *Int. J. Fruit Sci.*, 2020, **20**, S1662–S1680.
59 J. Dai and R. J. Mumper, *Molecules*, 2010, **15**, 7313–7352.
60 A. Wolnicka-Glubisz and A. Wisniewska-Becker, *Antioxidants*, 2023, **12**, 1725.